Taylor & Francis
Taylor & Francis Group

RESEARCH PAPER

Check for updates

Osthole inhibited TGF β-induced epithelial–mesenchymal transition (EMT) by suppressing NF-κB mediated Snail activation in lung cancer A549 cells

Haitao Feng [a], Jin-Jian Lu[a], Yitao Wang[a], Lixia Pei[b], and Xiuping Chen[a]

[a]State Key Laboratory of Quality Research in Chinese Medicine, Institute of Chinese Medical Sciences, University of Macau, Macau, China;
[b]Longhua Hospital, Shanghai University of Traditional Chinese Medicine, Shanghai, China

ABSTRACT

Epithelial-mesenchymal transition (EMT), the transdifferentiation of epithelial cells into mesenchymal cells, has been implicated in the metastasis and provides novel strategies for cancer therapy. Osthole (OST), a dominant active constituent of Chinese herb *Cnidium monnieri*, has been reported to inhibit cancer metastasis while the mechanisms remains unclear. Here, we studied the inhibitory effect and mechanisms of OST on TGF-β1-induced EMT in A549 cells. Cells were treated with TGF-β1 in the absence and presence of OST. The morphological alterations were observed with a microscopy. The protein and mRNA expressions were determined by Western blotting and real-time PCR. The protein localization was detected with immunofluorescence. The adhesion, migration, and invasion were determined by Matrigel, wound-healing, and Transwell assays. TGF-β1 treatment induced spindle-shaped alterations of cells, upregulation of N-cadherin, Vimentin, NF-κB p65, and downregulation of E-cadherin. Dysregulated membrane expression and mRNA expression of E-cadherin and N-cadherin were observed after TGF-β1 treatment. TGF-β1 increased abilities of migration and invasion and triggered the nuclear translocation of NF-κB p65. These alterations were dramatically inhibited by OST. Furthermore, PDTC, a NF-κB inhibitor, showed similar effects. In addition, TGF-β1-induced expression of Snail was significantly inhibited by OST and silenced Snail partially reversed TGF-β1-induced EMT biomarkers without affecting NF-κB p-65. In conclusion, OST inhibited TGF-β1-induced EMT, adhesion, migration, and invasion through inactivation of NF-κB-Snail pathways in A549 cells. This study provides novel molecular mechanisms for the anti-metastatic effect of OST.

Introduction

As known to all, cancer metastasis is the most common cause of cancer-related death in patients with solid tumors.[1] Lung cancer, the leading cause of cancer-related deaths, is prone to metastasis to brain and bone.,[2,3] Metastasis is a rather complicated process including several basic steps such as the detachment of tumor cells, invasion to surrounding tissues and basal lamina, crossing the basal lamina and entrance to the blood stream, transportation in the blood stream, and extravasation at a distal site and proliferation into a new foci.[4] A number of fundamental mechanisms such as cellular motility inducement,[5] lymphangiogenesis and angiogenesis,[6] degradation of matrix barriers,[7] tumor cell and endothelial cell interactions.[8] were required in metastasis.

Epithelial-mesenchymal transition (EMT) is a biological process characterized by loss of cell-cell junctions, polarity and epithelial markers, and in turn, acquisition of mesenchymal features and motility.[9,10] During this process, the immobile epithelial-like cancer cells switch to a motile mesenchymal-like phenotype thus resulting in alterations in morphology, cellular architecture, adhesion, and migration.[11,12] EMT is one of the key events in metastasis and often occurs at the invasive front of tumors.[13] Cancer-associated EMT also contributes to increased resistance to cell death, chemoresistance, bypass of senescence, immune system evasion and exhibition of cancer stem cell properties.[14-17] Therefore, the EMT pathways provide novel targets and potential strategies for anticancer therapy.[18,19]

Osthole (OST), a natural coumarin isolated from the Chinese herb Fructus Cnidii, showed various biological functions, such as neuroprotective, osteogenic, cardiovascular protective, immunomodulatory, hepatoprotective, and antimicrobial activities.[20] Furthermore, accumulating evidence indicated that OST possessed anti-tumor

activities by inhibiting tumor cell growth and inducing apoptosis.[21-24] It has been reported recently that OST inhibited the migration and invasion of various cancer cells *in vitro*.[25-28] However, the molecular mechanisms of these effects was not fully clarified. In the present study, we demonstrated a novel signal pathway involved in OST's inhibitory effect on TGF-β1-induced EMT in A549 lung cancer cells.

Materials and methods

Materials

OST (>98%) was purchased from Chengdu Preferred Biotech Co. Ltd. (Chengdu, China). Human recombinant TGF-β1 purchased from Cell Signaling Technology (Danvers, MA, USA) was activated and stored in accordance with the manufacturer's instructions. 3-(4,5-Dimethylthiazol-2-yl)-2,5-diphenyltetrazolium bromide (MTT), dimethylsulfoxide (DMSO), and Hoechst 33342 were purchased from Sigma-Aldrich (St. Louis, MO, USA). Antibodies for E-cadherin, N-cadherin, and Snail were purchased from Santa Cruz Biotechnology (Santa Cruz, CA, USA). Antibodies for GAPDH, NF-κB p65, phosphorylated-p65 (p-p65), IκBα, p-IκBα, Histone H3, and β-tubulin were purchased from Cell Signaling Technology (Danvers, MA, USA).

Cell culture

Human lung carcinoma epithelial cells A549 were cultured in RPMI 1640 medium supplemented with 10% (v/v) fetal bovine serum at 37°C in a humidified atmosphere of 5% CO_2 and 95% air.

MTT assay

Cells planted in 96-well plates (5×10^3 cells/well) were treated with OST (5–80 μM) for 48 h. Then 20 μl MTT (5 mg/ml) was added to each well and co-incubated for another 4 h. After removing the MTT-containing medium, 100 μl DMSO was added to solubilize the formazan. The absorbance at 570 nm was recorded using a microplate reader (PerkinElmer, USA).

Morphology observation

Cells (1×10^5) seeded in 12-well plates were treated with TGF-β1 (5 ng/ml) alone or in combination with OST (5–20 μM) for 48 h. The cells' morphology was captured by a bright-field microscope (IX73; Olympus, Japan).

Nuclear and cytoplasmic protein extraction

After exposure to TGF-β1 (5 ng/ml) with or without OST (20 μM) for 48 h, the nuclear and cytoplasmic proteins were prepared using Nuclear and Cytoplasmic Extraction Reagents (Thermo scientific, Rockford, IL, USA) according to the manufacturer's instructions.

Western blotting

Treated cells were collected and were lysed in RIPA buffer (50 mM Tris-HCl, 150 mM NaCl, 1% Nonidet P-40, 1% sodium deoxycholate, and 0.1% SDS, pH 8.0) containing a protease inhibitor cocktail and PMSF. Subsequently, the protein concentrations were determined using BCA™ Protein Assay Kit. The western blotting was performed as our previous report.[29]

Adhesion assay

Cells seeded in 12-well plates were incubated with TGF-β1 (5 ng/ml) alone or in combination with OST (5–20 μM) for 48 h. Then cells were harvested and seeded in Matrigel pre-coated 96-well plates. After 3 h, cells were labeled with crystal violet for 10 min in the dark. The non-adherent cells were washed mildly with PBS. Images were obtained under random fields of each well using a fluorescent microscopy (IN Cell Analyzer 2000, GE, USA).

Wound-healing assay

Cells (2×10^5 cells/well) were seeded in 6-well plates for 24 h and a cell-free line was manually created by scratching the confluent monolayers with a 100 μl pipette tip. The wounded monolayers were washed with PBS and cultured in RPMI1640 with 1% FBS containing TGF-β1 (5 ng/ml) alone or in combination with OST (5–20 μM) for 48 h. Five scratched fields were randomly chosen and the images were captured by a bright-field microscope (IX73; Olympus).

Invasion assay

Cells (2×10^5) plated in Matrigel-coated top chambers (8 nm pore size; Corning Inc., Corning, NY, USA) for 24 h. Cells were plated in serum-free medium (200 μl) and co-treated with TGF-β1 (5 ng/ml) and/or OST (5–20 μM). 500 μl normal medium with serum was used as chemoattractant in the lower chambers. The non-migrated cells were removed from the upper surface of the chamber after 24 h. Cells on the lower surface of the membrane were fixed with 4% paraformaldehyde

Table 1. Primers for RT-PCR assay.

Primers	Type	Sequence (5′to3′)
E-cadherin	forward	GCCTCCTGAAAAGAGAGTGGAAG
	reverse	TGGCAGTGTCTCTCCAAATCCG
N-cadherin	forward	ACAGTGGCCACCTACAAAGG
	reverse	CCGAGATGGGGTTGATAATG
Snail	forward	ACCACTATGCCGCGCTCTT
	reverse	GGTCGTAGGGCTGCTGGAA
GAPDH	forward	GCACCGTCAAGGCTGAGAAC
	reverse	TGG TGAAGACGCCAGTGGA

(PFA) and stained with crystal violet. The invading number of cells was counted under a bright-field microscope (×10, 3 random fields per well).

Quantitative real-time PCR

Treated cells were washed twice with PBS and the total RNA from each group was extracted with Trizol. The cDNA was synthesized using Takara reverse transcriptase and oligo (dT) primer from 2 μg of total RNA. Reverse transcription was performed at 37°C for 50 min followed by 15 min at 70°C for inactivation. Primer sequences were shown in Table 1. The PCR amplification were performed for 1 cycle of 95°C for 2 min, 40 cycles of 95°C for 15 s, 60°C for 30 s, and 1 cycle of 95°C for 30 s. The samples were assessed by $2^{-\Delta\Delta Ct}$ relative quantitative analysis to determine the expression differences.

Immunofluorescence assay

TGF-β1 (5 ng/ml) treated with or without OST co-treatment for 48 h were fixed with 4% PFA for 30 min. The immunofluorescence assay for E-cadherin, N-cadherin and NF-κB p65 were performed as our previous report.[29]

SiRNA silence

Cells were seeded in 6-well plates (1 × 10^6 cells/well) for overnight. The silence of Snail was performed as our previous report[30] using Lipofectamine3000 following manufacturer's instructions. The siRNA sequences for Snail were 5′-CAGAUGUCAAGAAGUACCATT-3′ and 5′-UGGUACUUCUUGACAUCUGTT-3′. The sequences for negative control were: 5′-UUCUCCGAACGUGUCAC-GUTT-3′ and 5′-ACGUGACACGUUCGGAGAATT-3′.

Statistical analysis

Data were expressed as the means ± SD. The differences between groups were analyzed using Prism 5.0 (Graph Pad Software Inc., San Diego, CA) and the statistical analysis was performed by analysis of variance (one-way ANOVA) followed by Student Newman-Keuls test. $p < 0.05$ is considered statistically significant.

Results

OST reversed TGF-β1-induced morphological changes

To avoid the effect of cell death on EMT, the cytotoxicity of OST and TGF-β1 alone or in combination was examined. As shown in Fig. 1A, OST showed no obvious cytotoxicity even at 20 μM but inhibited cell proliferation at 40 μM. TGF-β1 showed no cytotoxicity even at the concentration of 40 ng/ml (Fig. 1B). Furthermore, OST co-treatment with TGF-β1 showed no obvious cytotoxic effect on cell viability (Fig. 1C). TGF-β1 remarkably induced the mesenchymal phenotype in time- and dose-dependent manners. TGF-β1 treatment induced disappearance of intercellular junction and spindle-like appearance and demonstrating a fibroblast-like appearance with longed shape and central nucleus (Fig. 1D and E). These morphological alterations were obviously reversed by OST co-treatment (Fig. 1F).

OST reversed TGF-β1-induced expression of EMT biomarkers

TGF-β1 treatment significantly inhibited the protein expression of the epithelial marker E-cadherin and increased the mesenchymal marker N-cadherin and vimentin simultaneously in a time-dependent manner (Fig. 2A). These alterations were dramatically reversed by OST co-treatment in a concentration-dependent manner (Fig. 2B). Furthermore, the mRNA expression of E-cadherin and N-cadherin were downregulated and upregulated by TGF-β1, respectively, which was also partially restored by OST (Fig. 2C and D). Immunofluorescent staining results showed that intensive green fluorescence was observed on the membranes in the untreated cells suggesting the expression of E-cadherin, which was significantly decreased by TGF-β1 treatment. Co-treatment of OST partially reversed the E-cadherin expression (Fig. 2E). Similar reversible effect of OST was observed on TGF-β1-induced N-cadherin expression (Fig. 2F).

OST suppressed TGF-β1-induced migration and invasion

Compared with control or treated with OST alone, TGF-β1-treated cells showed enhanced migration
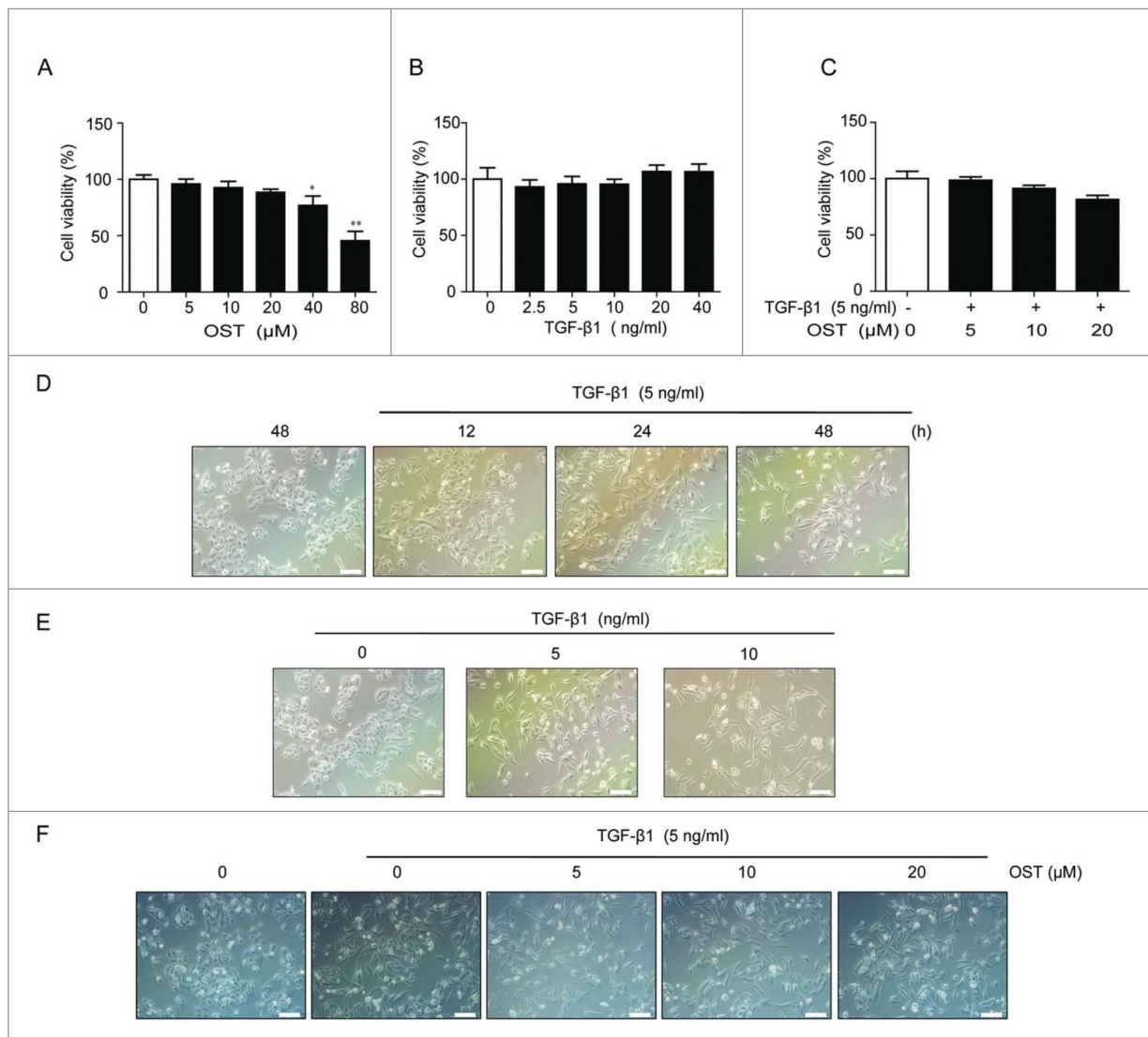
Figure 1. OST inhibited TGF-β1-induced morphological change. Cells were treated with OST (A) or TGF-β1 (B) or TGF-β1 (5 ng/ml) co-treated with OST (C) for 48 h and the cell viability was determined by MTT assay. Cells were treated with TGF-β1 for 48 h, the cell morphology was observed (D and E). Cells were treated with TGF-β1 (5 ng/ml) with or without OST co-treatment for 48 h and the cell morphology was observed (F). Scale bar = 100 μm. Magnification, $\times$20. $^*p < 0.05$ vs control, $^{**}p < 0.01$ vs control. OST, osthole.

activity in wound-healing assay, which was significantly inhibited by co-treated with OST (Fig. 3A). Furthermore, TGF-β1 promoted the invasion ability as evidenced by the increased number of migrated cells in Transwells assay, which was dramatically decreased by OST co-treatment (Fig. 3B). In addition, Matrigel assay results showed that TGF-β1 increased number of adhesion cells, which was significantly inhibited by OST as well (Fig. 3C).

OST inhibited TGF-β1-induced EMT mediated by NF-κB

To explore the role of NF-κB in OST-induced EMT, PDTC, a NF-κB inhibitor, was used. TGF-β1-induced morphological changes were partially reversed by PDTC

(Fig. 4A). PDTC co-treatment demonstrated similar regulatory effects on the expression of E-cadherin, N-cadherin, NF-κB p65, Snail, and vimentin to those of OST (Fig. 4B). Furthermore, PDTC pretreatment showed similar inhibitory effects on TGF-β1-induced migration, invasion, and adhesion to those of OST (Figs. 4C–E).

OST inhibited TGF-β1-induced IκBα degradation and p65 nuclear translocation

Immunofluorescent staining showed that compared with untreated cells, TGF-β1 treatment significantly increased the green fluorescence in the nuclear suggesting the increased expression of NF-κB p65 in nuclear. Co-treatment with OST significantly
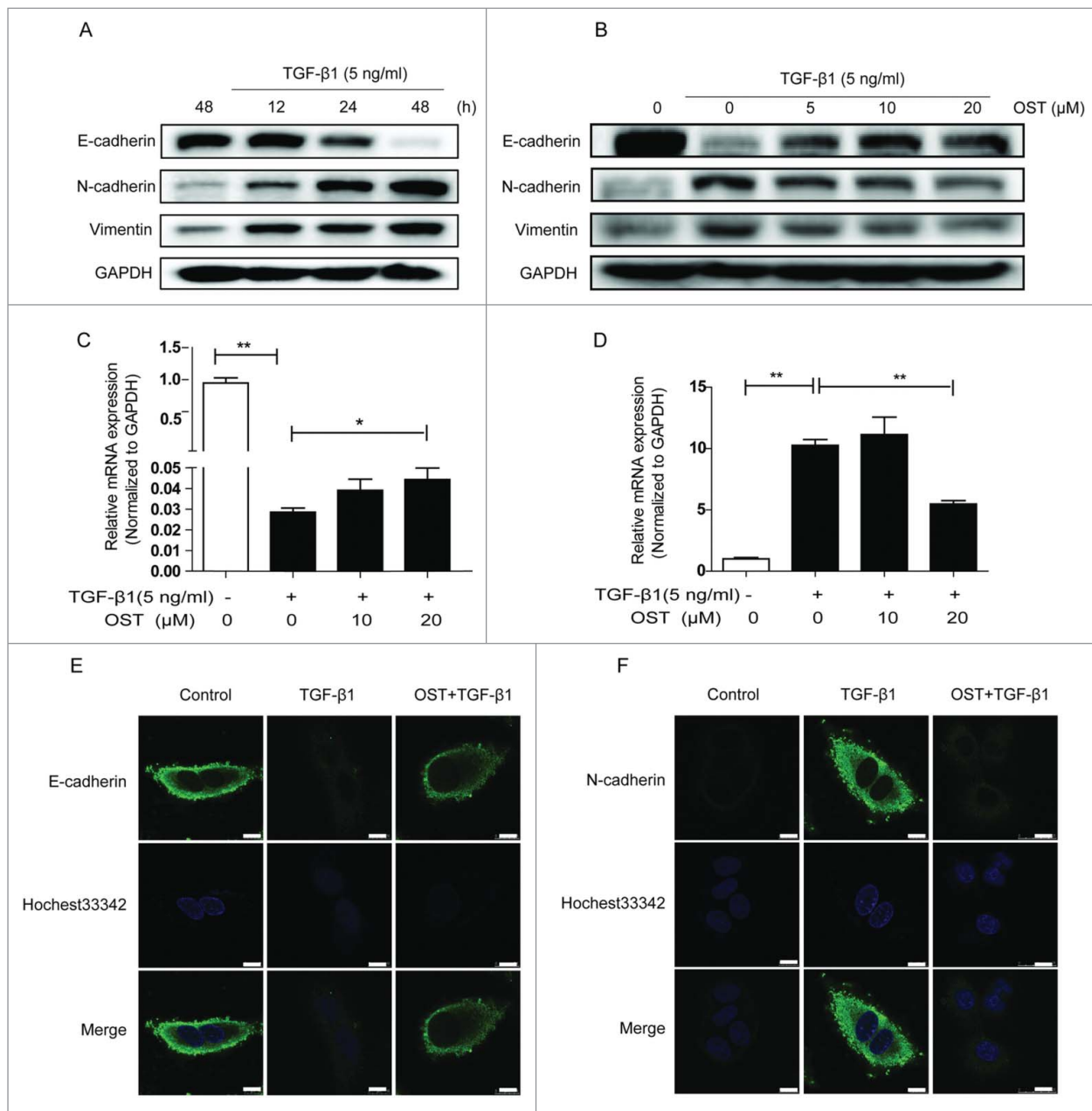
Figure 2. Effect of OST on the expression of EMT biomarkers. Cells were treated with TGF-β1 and the protein expression was determined by Western blotting (A). Cells were treated with TGF-β1 (5 ng/ml) for 48 h with or without OST co-treatment and the protein and mRNA expression were determined by Western blotting (B) and qRT-PCR (C and D), respectively. Immunofluorescence staining was performed for detecting the expression of E-cadherin (E) and N-cadherin. Scale bar = 10 μm. (F). $^{*}p < 0.05$ and $^{**}p < 0.01$. OST, osthole.

decreased the green fluorescence indicating that TGF-β1-induced nuclear translocation of NF-κB p65 was inhibited (Fig. 5A). Furthermore, Western blotting showed that after TGF-β1 stimulation, the expression of NF-κB p65 in cytoplasmic extracts was decreased (Fig. 5B) while its expression in the nuclear was increased (Fig. 5C). OST treatment could partially reverse these effects. In addition, increased phosphorylation of IκBα by TGF-β1 was also partially inhibited by OST (Fig. 5B).

Snail mediated TGF-β1-induced EMT

TGF-β1 treatment significantly increased the protein expression of Snail in a time-dependent manner (Fig 6A), which was dramatically decreased by OST in a dose-dependent manner (Fig 6B). The qRT-PCR results showed that TGF-β1-induced increase of Snail was suppressed by OST (Fig 6C). Furthermore, compared with the control, silencing Snail by siRNA (Fig 6D) dramatically reversed TGF-β1-induced dysregulation of
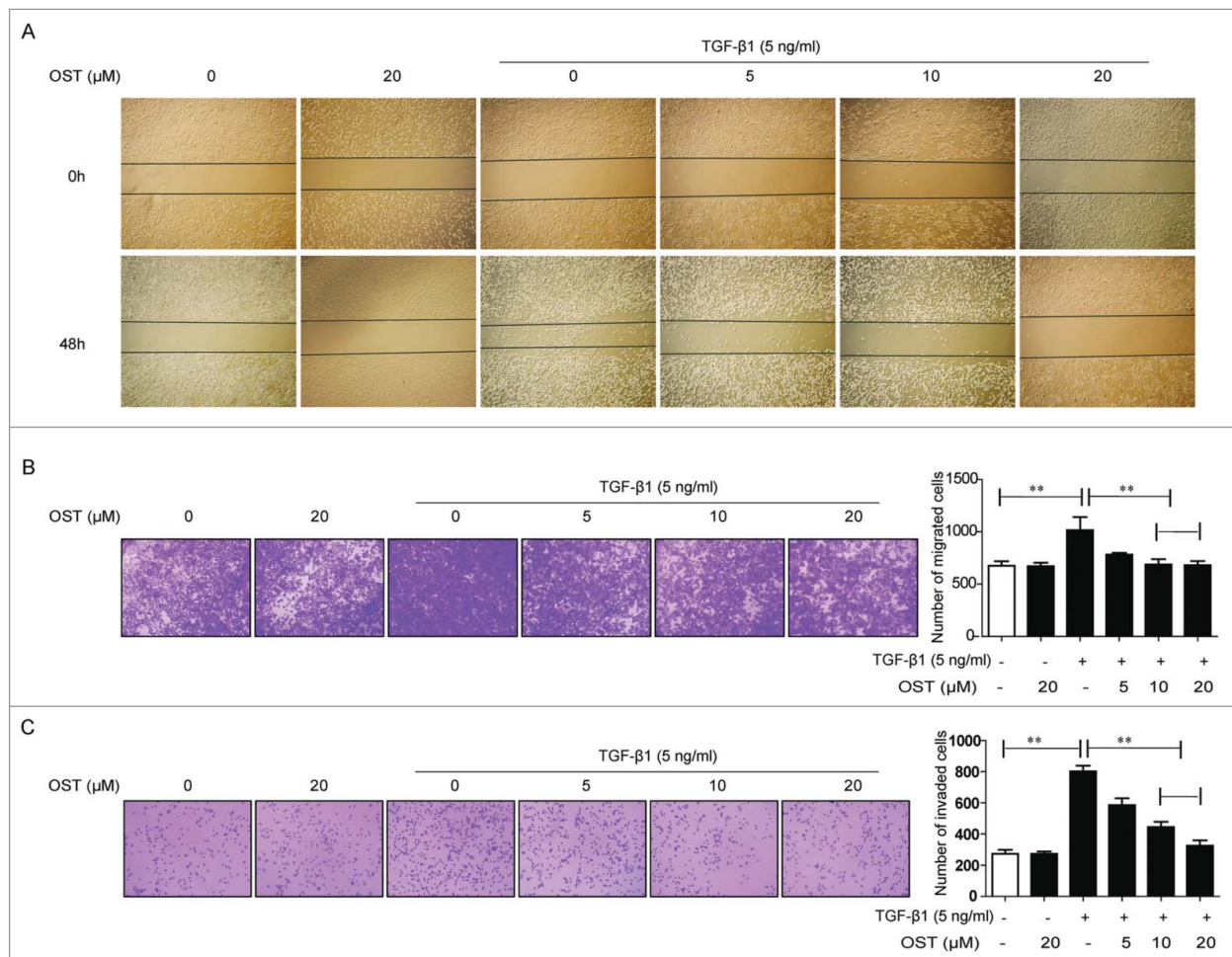
Figure 3. OST inhibited TGF-β1-induced migration, invasion, and adhesion. Cells were treated with TGF-β1 (5 ng/ml) with or without OST co-treatment for 48 h. The migration, invasion, and adhesion capacities were measured by the wound healing (Magnification, $\times$4) (A), Transwell (Magnification, $\times$10) (B), and Matrigel (Magnification, $\times$10) (C) assay, respectively. $^{**}p < 0.01$. OST, osthole.

E-cadherin, N-cadherin, and vimentin while showed no effect on NF-κB p65 (Fig 6E).

Discussion

Accumulated data showed the anticancer effect of OST by induction of cell cycle arrest,[25,31] apoptosis,[22,24] and inhibition of invasion and migration.[25,27,32] In this study, the anti-metastatic effect of OST was investigated. The main findings were: 1). OST inhibited TGF-β1-induced EMT in A549 cells. 2). OST inhibited TGF-β1-induced A549 cells invasion, migration, and adhesion. 3). Inhibition of Snail mediated by inactivation of NF-κB was the underlying mechanisms.

EMT is characterized by the morphological alterations in cell shape and the biochemical changes of the downregulation of epithelial markers (E-cadherin, ZO-1, and β-catenin) and the upregulation of mesenchymal markers (N-cadherin and vimentin).[12,33] Our results showed that the epithelial phenotype of A549 cells gradually transferred to mesenchymal phenotype in response to TGF-β1 treatment suggesting that EMT occurred. This was further confirmed by the downregulation of E-cadherin and the upregulation of N-cadherin both at protein and mRNA levels. Vimentin, a protein ubiquitously expressed in normal mesenchymal cells, has also been recognized as a biomarker for EMT.[34] The activation of vimentin and the membrane localization of E-cadherin and N-cadherin provided further evidence for the occurrence of EMT. Increased EMT promote cancer progress by increasing tumor cell adhesion, invasion, and migration. Here, we found that TGF-β1 significantly enhanced the migration, invasion, and adhesion as evidenced by the increased ability of A549 cells in response to TGF-β1 in the wound healing, Transwell, and Matrigel assays. Thus, these increased cell mobility in response to TGF-β1 was resulted from, at least in part, EMT in A549 cells.
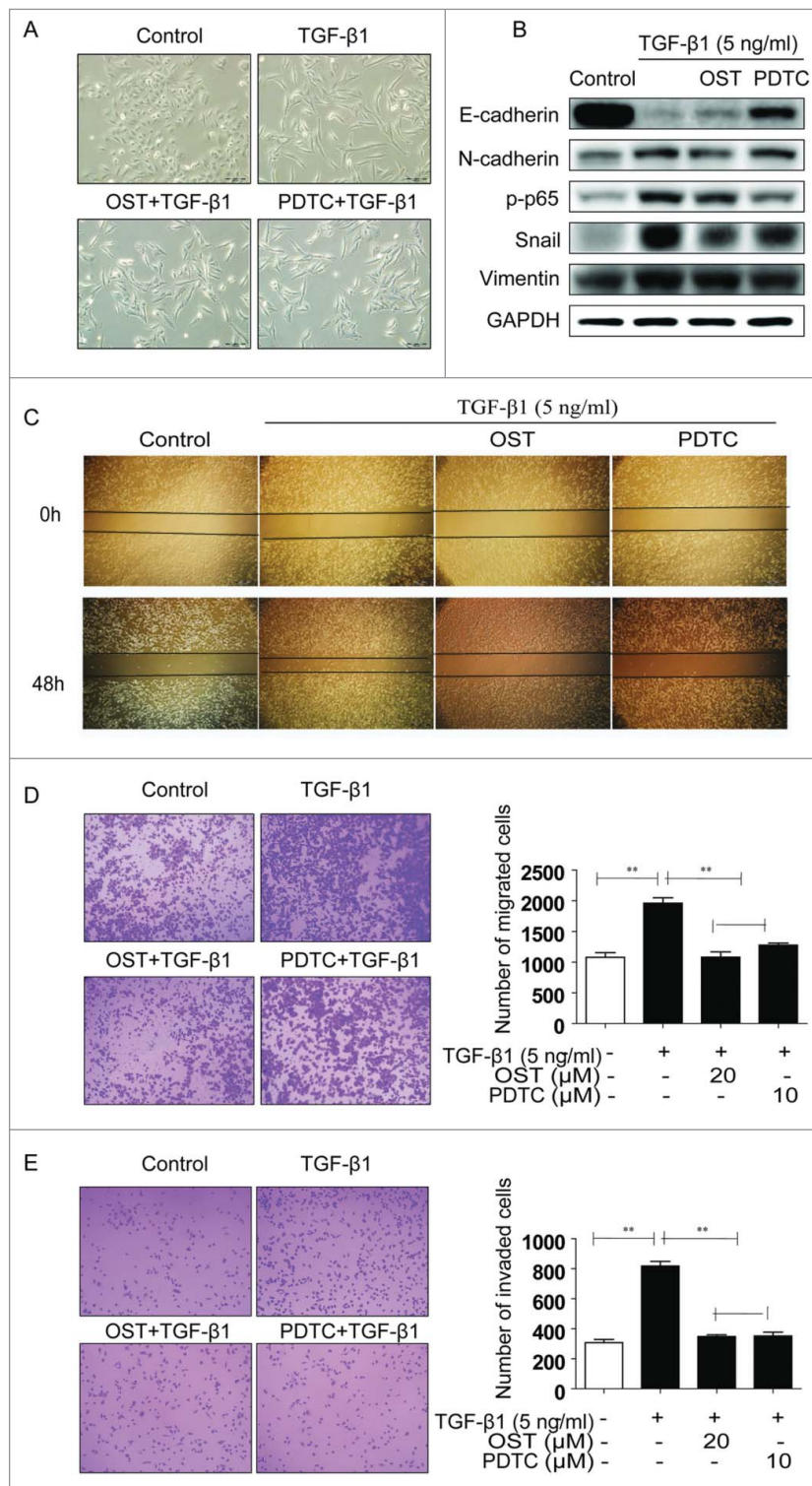
Figure 4. OST inhibited EMT through inactivation of NF-κB signaling. Cells were treated with TGF-β1 (5 ng/ml) alone or co-treatment with OST (20 μM) or PDTC (10 μM) for 48 h and the morphological changes (Magnification, ×20) (A), the protein expression were detected (B). Cells were treated with TGF-β1 with or without PDTC co-treatment for 48 h and the migration, invasion, and adhesion capacities were measured by the wound healing (Magnification, ×4) (C), Transwell (Magnification, ×10) (D), and Matrigel (Magnification, ×10) (E) assay, respectively. $^{**}p < 0.01$. OST, osthole.

Previous studies have suggested that NF-κB played an essential role in TGF-β1-induced EMT.[35,36] Involvement of NF-κB pathways in TGF-β1-induced EMT in A549

cells was also documented.[37] Consistent with previous report,[38] TGF-β1-induced nuclear translocation of p65 was observed in immunofluorescence assay. This was
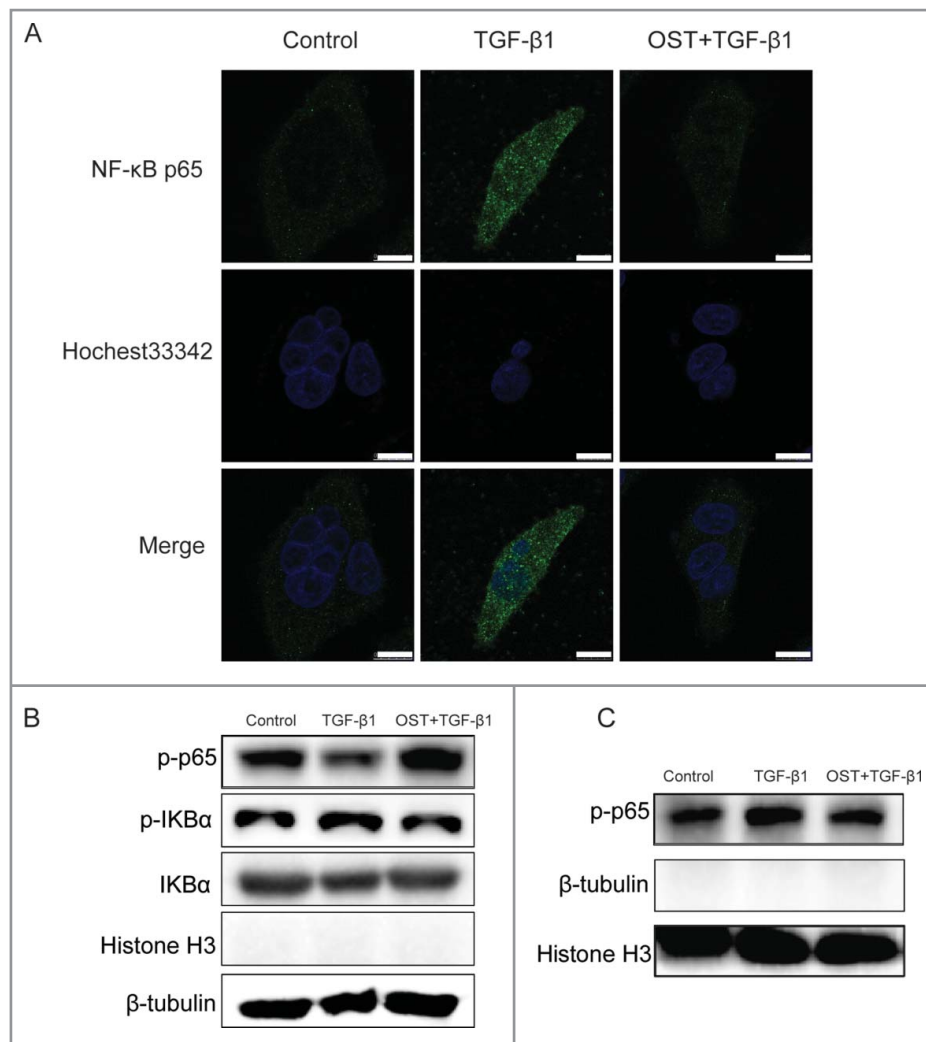
Figure 5. OST suppressed TGF-β1-induced NF-κB nuclear translocation. Cells were treated with TGF-β1 (5 ng/mL) in the absence or presence of OST for 48 h and the expression of p65 was determined by immunofluorescence assay. Scale bar = 10 μm. (A). The cytosolic (B) and nuclear (C) protein expression of p-p65, IκBα, and p-IκBα were detected by Western blotting. OST, osthole.

further confirmed by the decreased cytoplasm expression and increased nuclear expression. Activation of NF-κB involves the phosphorylation, ubiquitination, and degradation of IκBα and the phosphorylation of p65, which leads to translocation of NF-κB p65 to the nucleus, where it binds to specific response elements in the DNA.[39] The increased phosphorylation of IκBα suggested that TGF-β1 promote p65 translocation by phosphorylation of IκBα. Thus, the NF-κB pathway played a key role in TGF-β1-induced EMT under our experimental conditions. The inhibitory effect of PDTC, a NF-κB inhibitor, on TGF-β1-induced morphological alterations, switch of EMT biomarkers, adhesion, migration, and invasion, further confirmed this. Various transcription factors, including Snail, a zinc finger transcription factor, has been reported to modulate EMT.[40,41] Snail binds to the promoter of the E-cadherin gene and suppresses its transcription, which is one of the hallmarks of EMT and

metastasis.[42,43] TGF-β1-induced Snail expression was inhibited by PDTC while silence Snail showed no effect on p65 expression suggesting that Snail might be regulated by NF-κB pathway. Furthermore, the regulation of EMT biomarkers by Snail siRNA revealed the participation of Snail in TGF-β1-induced EMT. Thus, NF-κB mediated Snail activation played potential roles in TGF-β1-induced EMT in A549 cells.

The inhibitory effect of OST, a natural product, on EMT has been reported. OST inhibited EMT induced by TGF-β1, insulin-like growth factor-1, and hepatocyte growth factor in prostate cancer cells,[44] GBM8401 cells,[45] and MCF-7 cells,[46] respectively. The underlying mechanisms included inhibition of Snail signaling and miR-23a-3p,[44] inhibition of PI3K/Akt[45] and repression of c-Met/Akt/mTOR pathway.[46] In this study, OST partially reversed TGF-β1-induced morphological changes, expression of EMT biomarkers suggesting that OST inhibited
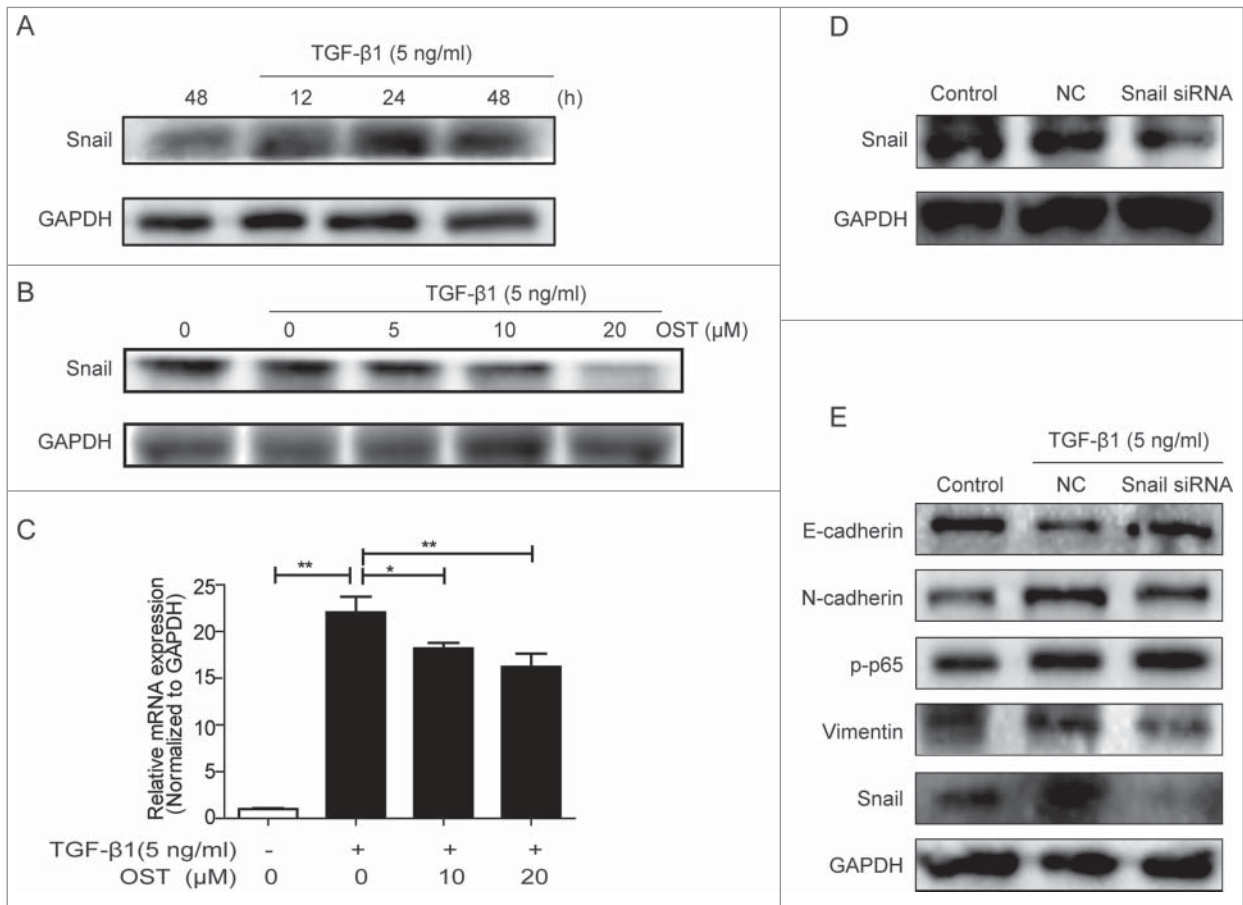
Figure 6. Snail involved in TGF-β1-induced EMT Cells were treated with TGF-β1 in the absence or presence of OST co-treatment and the protein and mRNA expressions of Snail were determined by Western blotting (A and B) and qRT-PCR (C). Snail was silenced with siRNA (D) and then treated with TGF-β1 (5 ng/ml) for 48 h, the protein expression was determined by Western blotting. $^*p < 0.05$, $^{**}p < 0.01$. OST, osthole.

TGF-β1-induced EMT in A549 cells. The inhibitory effect of OST on TGF - β1-induced adhesion, migration, and invasion indicated that OST might have anti-metastatic effect by suppressing EMT. Furthermore, OST showed similar inhibitory effect to that of PDTC on TGF-β1-induced alterations morphologically and biochemically. Thus, it suggested that OST inhibited EMT by modulation of NF-κB pathway. Along with its downregulation of Snail, the inhibitory effect of OST was probably mediated by inactivation of NF-κB-Snail signal pathway.
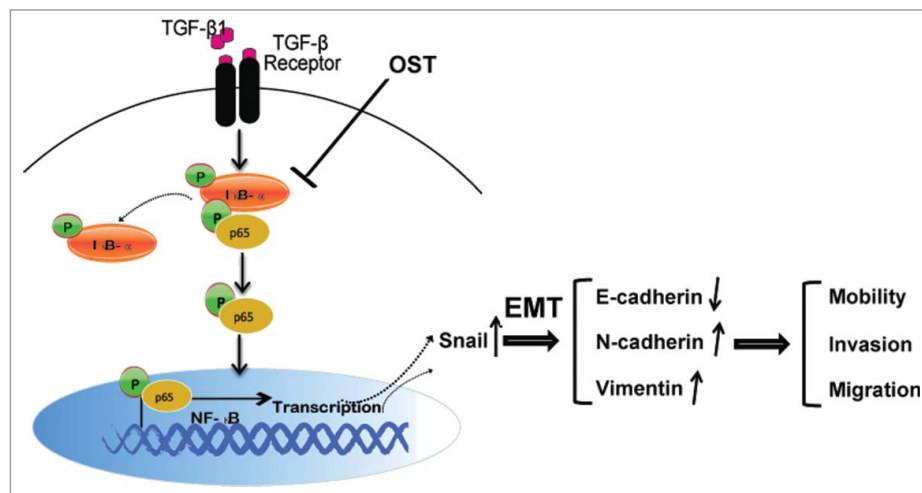

Figure 7. OST inhibited TGF-β1-induced EMT in A549 cells.

In summary, as depicted in Fig. 7, the study demonstrated that OST inhibited TGF-β1-induced EMT, adhesion, invasion and migration in A549 cells possibly through downregulating NF-κB-Snail pathways. These findings shed new insights into the anti-metastatic effect of OST.

Disclosure of potential conflicts of interest

No potential conflicts of interest were disclosed.

Funding

ORCID

Haitao Feng http://orcid.org/0000-0003-1518-8336

References

[1] Coleman RE. Clinical features of metastatic bone disease and risk of skeletal morbidity. Clin Cancer Res 2006; 12:6243s-9s; PMID:17062708; https://doi.org/10.1158/1078-0432.CCR-06-0931

[2] Hanibuchi M, Kim SJ, Fidler IJ, Nishioka Y. The molecular biology of lung cancer brain metastasis: an overview of current comprehensions and future perspectives. J Med Invest 2014; 61:241-53; PMID:25264041; https://doi.org/10.2152/jmi.61.241

[3] D'Antonio C, Passaro A, Gori B, Del Signore E, Migliorino MR, Ricciardi S, Fulvi A, de Marinis F. Bone and brain metastasis in lung cancer: recent advances in therapeutic strategies. Therap Adv Med Oncol 2014; 6:101-14; PMID:24790650; https://doi.org/10.1177/1758834014521110

[4] Perlikos F, Harrington KJ, Syrigos KN. Key molecular mechanisms in lung cancer invasion and metastasis: a comprehensive review. Critic Rev Oncol/Hematol 2013; 87:1-11; PMID:23332547; https://doi.org/10.1016/j.critrevonc.2012.12.007

[5] Wells A, Grahovac J, Wheeler S, Ma B, Lauffenburger D. Targeting tumor cell motility as a strategy against invasion and metastasis. Trends Pharmacol Sci 2013; 34:283-9; PMID:23571046; https://doi.org/10.1016/j.tips.2013.03.001

[6] Paduch R. The role of lymphangiogenesis and angiogenesis in tumor metastasis. Cell Oncol (Dordrecht) 2016; 39:397-410.

[7] Jiang D, Lim SY. Influence of immune myeloid cells on the extracellular matrix during cancer metastasis. Cancer Microenviron 2016; 9:45-61.

[8] Reymond N, d'Agua BB, Ridley AJ. Crossing the endothelial barrier during metastasis. Nat Rev Cancer 2013; 13:858-70; PMID:24263189; https://doi.org/10.1038/nrc3628

[9] Seton-Rogers S. Epithelial-mesenchymal transition: Untangling EMT's functions. Nat Rev Cancer 2016; 16:1; PMID:26612535; https://doi.org/10.1038/nrc.2015.6

[10] Li L, Li W. Epithelial-mesenchymal transition in human cancer: comprehensive reprogramming of metabolism, epigenetics, and differentiation. Pharmacol Therapeut 2015; 150:33-46; PMID:25595324; https://doi.org/10.1016/j.pharmthera.2015.01.004

[11] Lin Y-C, Lin J-C, Hung C-M, Chen Y, Liu L-C, Chang T-C, Kao JY, Ho CT, Way TD. Osthole inhibits insulin-like growth factor-1-induced epithelial to mesenchymal transition via the inhibition of PI3K/Akt signaling pathway in human brain cancer cells. J Agricul Food Chem 2014; 62:5061-71; PMID:24828835; https://doi.org/10.1021/jf501047g

[12] Gonzalez DM, Medici D. Signaling mechanisms of the epithelial-mesenchymal transition. Sci Signal 2014; 7:re8; PMID:25249658; https://doi.org/10.1126/scisignal.2005189

[13] Wen Y-C, Lee W-J, Tan P, Yang S-F, Hsiao M, Lee L-M, Chien MH. By inhibiting snail signaling and miR-23a-3p, osthole suppresses the EMT-mediated metastatic ability in prostate cancer. Oncotarget 2015; 6:21120; PMID:26110567; https://doi.org/10.18632/oncotarget.4229

[14] Micalizzi DS, Farabaugh SM, Ford HL. Epithelial-mesenchymal transition in cancer: parallels between normal development and tumor progression. J Mammary Gland Biol Neoplasia 2010; 15:117-34; PMID:20490631; https://doi.org/10.1007/s10911-010-9178-9

[15] Reiman JM, Knutson KL, Radisky DC. Immune promotion of epithelial-mesenchymal transition and generation of breast cancer stem cells. Cancer Res 2010; 70:3005-8; PMID:20395197; https://doi.org/10.1158/0008-5472.CAN-09-4041

[16] Stallings-Mann ML, Waldmann J, Zhang Y, Miller E, Gauthier ML, Visscher DW, Downey GP, Radisky ES, Fields AP, Radisky DC. Matrix metalloproteinase induction of Rac1b, a key effector of lung cancer progression. Sci Translat Med 2012; 4:142ra95-ra95; PMID:22786680; https://doi.org/10.1126/scitranslmed.3004062

[17] Thiery JP, Acloque H, Huang RY, Nieto MA. Epithelial-mesenchymal transitions in development and disease. Cell 2009; 139:871-90; PMID:19945376; https://doi.org/10.1016/j.cell.2009.11.007

[18] Huang RY, Chung VY, Thiery JP. Targeting pathways contributing to epithelial-mesenchymal transition (EMT) in epithelial ovarian cancer. Curr Drug Targets 2012; 13:1649-53; PMID:23061545; https://doi.org/10.2174/1389450012803530044

[19] Davis FM, Stewart TA, Thompson EW, Monteith GR. Targeting EMT in cancer: opportunities for pharmacological intervention. Trends Pharmacol Sci 2014; 35:479-88; PMID:25042456; https://doi.org/10.1016/j.tips.2014.06.006

[20] Zhang ZR, Leung WN, Cheung HY, Chan CW. Osthole: A review on its bioactivities, pharmacological properties, and potential as alternative medicine. Evid Based Complement Alternat Med 2015; 2015:919616; PMID:26246843

[21] Chou SY, Hsu CS, Wang KT, Wang MC, Wang CC. Antitumor effects of Osthol from Cnidium monnieri: an

in vitro and in vivo study. Phytother Res 2007; 21:226-30; PMID:17154232; https://doi.org/10.1002/ptr.2044

[22] Xu X, Zhang Y, Qu D, Jiang T, Li S. Osthole induces G2/M arrest and apoptosis in lung cancer A549 cells by modulating PI3K/Akt pathway. J Exp Clin Cancer Res 2011; 30:1; PMID:21208462; https://doi.org/10.1186/1756-9966-30-1

[23] Jarzab A, Grabarska A, Kielbus M, Jeleniewicz W, Dmoszynska-Graniczka M, Skalicka-Wozniak K, Sieniawska E, Polberg K, Stepulak A. Osthole induces apoptosis, suppresses cell-cycle progression and proliferation of cancer cells. Anticancer Res 2014; 34:6473-80; PMID:25368248

[24] Wang L, Peng Y, Shi K, Wang H, Lu J, Li Y, Ma C. Osthole inhibits proliferation of human breast cancer cells by inducing cell cycle arrest and apoptosis. J Biomed Res 2015; 29:132-8; PMID:25859268

[25] Wang L, Yang L, Lu Y, Chen Y, Liu T, Peng Y, Zhou Y, Cao Y, Bi Z, Liu T. Osthole induces cell cycle arrest and inhibits migration and invasion via PTEN/Akt Pathways in Osteosarcoma. Cell Physiol Biochem 2016; 38:2173-82; PMID:27185245; https://doi.org/10.1159/000445573

[26] Kao SJ, Su JL, Chen CK, Yu MC, Bai KJ, Chang JH, Bien MY, Yang SF, Chien MH. Osthole inhibits the invasive ability of human lung adenocarcinoma cells via suppression of NF-kappaB-mediated matrix metalloproteinase-9 expression. Toxicol Appl Pharmacol 2012; 261:105-15; PMID:22503731; https://doi.org/10.1016/j.taap.2012.03.020

[27] Xu XM, Zhang Y, Qu D, Feng XW, Chen Y, Zhao L. Osthole suppresses migration and invasion of A549 human lung cancer cells through inhibition of matrix metalloproteinase-2 and matrix metallopeptidase-9 in vitro. Mol Med Rep 2012; 6:1018-22; PMID:22923177

[28] Tsai CF, Yeh WL, Chen JH, Lin C, Huang SS, Lu DY. Osthole suppresses the migratory ability of human glioblastoma multiforme cells via inhibition of focal adhesion kinase-mediated matrix metalloproteinase-13 expression. Internat J Mol Sci 2014; 15:3889-903; PMID:24599080; https://doi.org/10.3390/ijms15033889

[29] Haitao F, Wenwen Z, Jin-Jian L, Yitao W, Chen. X. Hypaconitine inhibits TGF-β1-induced epithelial-mesenchymal transition and suppresses adhesion, migration, and invasion in A549 lung cancer cells. Chinese J Nat Med 2016; in press.

[30] Zhao W, Ma G, Chen X. Lipopolysaccharide induced LOX-1 expression via TLR4/MyD88/ROS activated p38MAPK-NF-kappaB pathway. Vascular Pharmacol 2014; 63:162-72; PMID:25135647; https://doi.org/10.1016/j.vph.2014.06.008

[31] Wang L, Peng Y, Shi K, Wang H, Lu J, Li Y, Ma C. Osthole inhibits proliferation of human breast cancer cells by inducing cell cycle arrest and apoptosis. J Biomed Res 2015; 29:132; PMID:25859268

[32] Xu X-M, Zhang Y, Qu D, Feng X-W, Chen Y, Zhao L. Osthole suppresses migration and invasion of A549 human lung cancer cells through inhibition of matrix metalloproteinase-2 and matrix metallopeptidase-9 in vitro. Mol Med Rep 2012; 6:1018-22; PMID:22923177

[33] Thiery JP. Epithelial–mesenchymal transitions in tumour progression. Nat Rev Cancer 2002; 2:442-54; PMID:12189386; https://doi.org/10.1038/nrc822

[34] Satelli A, Li S. Vimentin in cancer and its potential as a molecular target for cancer therapy. Cell Mol Life Sci 2011; 68:3033-46; PMID:21637948; https://doi.org/10.1007/s00018-011-0735-1

[35] Huber MA, Azoitei N, Baumann B, Grunert S, Sommer A, Pehamberger H, Kraut N, Beug H, Wirth T. NF-kappaB is essential for epithelial-mesenchymal transition and metastasis in a model of breast cancer progression. J Clin Invest 2004; 114:569-81; PMID:15314694; https://doi.org/10.1172/JCI200421358

[36] Min C, Eddy SF, Sherr DH, Sonenshein GE. NF-kappaB and epithelial to mesenchymal transition of cancer. J Cell Biochem 2008; 104:733-44; PMID:18253935; https://doi.org/10.1002/jcb.21695

[37] Borthwick LA, Gardner A, De Soyza A, Mann DA, Fisher AJ. Transforming Growth Factor-beta1 (TGF-beta1) Driven Epithelial to Mesenchymal Transition (EMT) is Accentuated by Tumour Necrosis Factor alpha (TNFalpha) via Crosstalk Between the SMAD and NF-kappaB Pathways. Cancer Microenvir 2012; 5:45-57; PMID:21792635; https://doi.org/10.1007/s12307-011-0080-9

[38] Cheng HH, Chu LY, Chiang LY, Chen HL, Kuo CC, Wu KK. Inhibition of cancer cell epithelial mesenchymal transition by normal fibroblasts via production of 5-methoxytryptophan. Oncotarget 2016; 7:3143–56.

[39] Karin M, Ben-Neriah Y. Phosphorylation meets ubiquitination: the control of NF-κB activity. Annu Rev Immunol 2000; 18:621-63; PMID:10837071; https://doi.org/10.1146/annurev.immunol.18.1.621

[40] Willis BC, Borok Z. TGF-β-induced EMT: mechanisms and implications for fibrotic lung disease. Am J Physiol-Lung Cell Mol Physiol 2007; 293:L525-L34; PMID:17631612; https://doi.org/10.1152/ajplung.00163.2007

[41] Zeisberg M, Neilson EG. Biomarkers for epithelial-mesenchymal transitions. J Clin Invest 2009; 119:1429-37; PMID:19487819; https://doi.org/10.1172/JCI36183

[42] Dong C, Wu Y, Yao J, Wang Y, Yu Y, Rychahou PG, Evers BM, Zhou BP. G9a interacts with Snail and is critical for Snail-mediated E-cadherin repression in human breast cancer. J Clin Invest 2012; 122:1469-86; PMID:22406531; https://doi.org/10.1172/JCI57349

[43] Jin H, Yu Y, Zhang T, Zhou X, Zhou J, Jia L, Wu Y, Zhou BP, Feng Y. Snail is critical for tumor growth and metastasis of ovarian carcinoma. Internat J Cancer 2010; 126:2102-11; PMID:19795442

[44] Wen YC, Lee WJ, Tan P, Yang SF, Hsiao M, Lee LM, Chien MH. By inhibiting snail signaling and miR-23a-3p, osthole suppresses the EMT-mediated metastatic ability in prostate cancer. Oncotarget 2015; 6:21120-36; PMID:26110567; https://doi.org/10.18632/oncotarget.4229

[45] Lin YC, Lin JC, Hung CM, Chen Y, Liu LC, Chang TC, Kao JY, Ho CT, Way TD. Osthole inhibits insulin-like growth factor-1-induced epithelial to mesenchymal transition via the

inhibition of PI3K/Akt signaling pathway in human brain cancer cells. J Agri Food Chem 2014; 62:5061-71; PMID:24828835; https://doi.org/10.1021/jf501047g

[46] Hung CM, Kuo DH, Chou CH, Su YC, Ho CT, Way TD. Osthole suppresses hepatocyte growth factor (HGF)-induced epithelial-mesenchymal transition via repression of the c-Met/Akt/mTOR pathway in human breast cancer cells. J Agri Food Chem 2011; 59:9683-90; PMID:21806057; https://doi.org/10.1021/jf2021489